# Turning Dynamics and Equilibrium of Two-Wheeled Vehicles

**Chih-Keng Chen*, Thanh-Son Dao, Chih-Kai Yang**
*Department of Mechanical and Automation Engineering, Da-Yeh University, 112 Shan-Jiau Rd., Changhua, Taiwan 515 ROC*

The equations of motion of two-wheeled vehicles, e.g. bicycles or motorcycles, are developed by using Lagrange's equations for quasi-coordinates. The pure rolling constraints between the ground and the two wheels are considered in the dynamical equations of the system. For each wheel, two nonholonomic and two holonomic constraints are introduced in a set of differential-algebraic equations (DAE). The constraint Jacobian matrix is obtained by collecting all the constraint equations and converting them into the velocity form. Equilibrium, an algorithm for searching for equilibrium points of two-wheeled vehicles and the associated problems are discussed. Formulae for calculating the radii of curvatures of ground-wheel contact paths and the reference point are also given.

**Key Words :** Bicycle Dynamics, Two-Wheeled Vehicle, Nonholonomic Constraint, Multibody

## 1. Introduction

Due to the challenges in fully understanding their dynamics and stabilization, two-wheeled vehicles have been attracting a considerable concern from a number of researchers in the fields of physics, automation and control. Alleyne et al.(1997) provided both simulation and experimental views at lateral vehicle dynamics for automatic steering control. Beznos et al.(1998) modeled a bicycle with gyroscopes that enabled the vehicle to stabilize itself on an autonomous motion along a straight line as well as along a curve. In their study, the stabilization unit consisted of two coupled gyroscopes spinning in opposite directions. Chen et al.(1998) provided an approach to decoupling the yaw motion from the lateral motion by using yaw rate feedback. Feng et al. (1998) applied $H_\infty$ theory and a three-degree-of-freedom (DOF) model for synthesis of robust steering controllers for a bicycle. Getz et al. (1993 ; 1995) derived a controller using steering and rear-wheel torques to make their unmanned bicycle maintain its balance, and, when the steering angle and rear-wheel velocities are non-zero, designed a feedback control method to control the bicycle to track arbitrary smooth trajectories with nonholonomic constraints and nonminimum phases. Discussions about internal equilibrium control applied to the path-tracking with balance using steering and rear-wheel torques as inputs were also given. Yao et al.(1994) presented a kinetic-model-based algorithm for estimating some unstabilized components in vehicular motion. In a study of Suryanaryanan et al.(2002), the system dynamics and automated roll-rate control of front and rear-wheel steered bicycles were proposed. Yavin (1997 ; 1999) dealt with the stabilization and control of a riderless bicycle by using a pedalling torque, a directional torque and a rotor mounted on the crossbar that generated a tilting torque. In another study (Indiveri, 1999), a closed loop, time-invariant and globally stable control law for a bicycle-like kinematic model was introduced. Lee et al.(2002) built a simple kinematic and dynamic formulation of an unmanned electric bicycle with a load mass balance

* Corresponding Author,
**E-mail** : ckchen@mail.dyu.edu.tw
**TEL** : +82-886-4-8511888; **FAX** : +886-4-8511224
Department of Mechanical and Automation Engineering, Da-Yeh University, 112 Shan-Jiau Rd., Changhua, Taiwan 515 ROC. (Manuscript **Received** November 29, 2004; **Revised** December 15, 2004)

system. He also proposed a control algorithm for self-stabilization using nonlinear control and then, implemented simulations of straight driving and turning of vehicular motions.

Most previous studies dealt with simplified mathematical models of two-wheeled vehicles which then were used to implement simulations, analysis and experiments. However, due to their simplicity, the mathematical models were unable to present all of the dynamic motions of the system in some situations. With that in mind, we approach by modeling a two-wheeled vehicle as a nine DOF system in three-dimensional space by using Lagrange's equations for quasi-coordinates. Also, the constraints equations are derived from wheel-ground contact conditions.

This paper is organized as follows : In Section 2, the nine DOF model describing the motion of two-wheeled vehicles is obtained by Lagrange's method. Constraint conditions between wheels and the ground are discussed in Section 3. Section 4 deals with equilibrium of two-wheeled vehicles and introduces a strategy for equilibrium points search, along with some selected numerical results. Formulae for calculating the radii of curvatures of ground-wheel contact paths and the reference point are also given. In Section 5 are some concluding remarks.

## 2. Three-Dimensional Two-Wheeled Vehicle Model

In this section, the compact equations of motion with nine degrees of freedom are developed to describe the dynamics of two-wheeled vehicles. The equations discussed here are developed by Lagrange's equations for quasi-coordinates (Baruh, 1999).

### 2.1 Coordinate systems

The schematic of a typical two-wheeled vehicle model is shown in Fig. 1. Let the uppercase letters $A$. $B$, $D$ and $F$ represent the vehicle body, the rear wheel, the front wheel and the fork, respectively, while the lowercase ones $a$, $b$, $d$, and $f$ are used to designate the center of mass of each part. Reference point $c$ is between

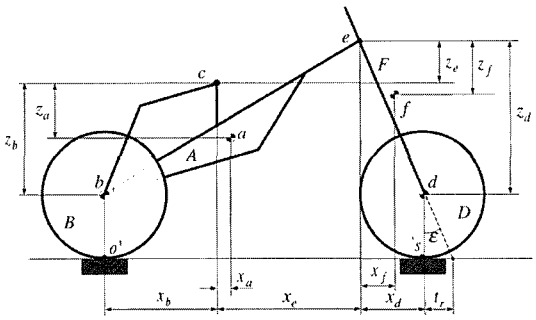


(a)

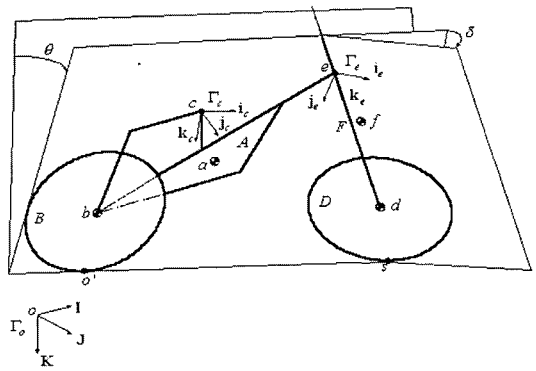


(b)

**Fig. 1** Two-wheeled vehicle model

the saddle and the vehicle body ; $e$ is a point between the vehicle body and the front fork ; $o'$ and $s$ are the contact points between the ground and the rear and front wheels, respectively.

There are three SAE-standard coordinate systems used in the model : (1) an inertial frame $\Gamma_o(\mathbf{I}, \mathbf{J}, \mathbf{K})$ fixed on the ground, (2) a reference frame $\Gamma_c(\mathbf{i}_c, \mathbf{j}_c, \mathbf{k}_c)$ mounted on the model at point $c$, and (3) a frame $\Gamma_e(\mathbf{i}_e, \mathbf{je}, \mathbf{ke})$ placed on the front fork at point $e$. The coordinate $\Gamma_e$ is obtained by rotating about $\Gamma_c$ a rake angle $\varepsilon$ and a steering angle $\delta$ as shown in Fig. 1. In this paper the dynamics of two-wheeled vehicles is described by the motion of the reference point $c$. Six coordinates are used to designate the positions and orientations of point $c$. The other three coordinate variables are the rotating angles of the front and rear wheels and the steering angle of the front fork. According to the foregoing definitions, the generalized coordinates can be written as

$$\mathbf{q}=[X\ Y\ Z\ \psi\ \phi\ \theta\ \delta\ \phi_r\ \phi_f]^T$$

where $(X, Y, Z)$ are the position parameters and

$(\psi, \phi, \theta)$ are the three Euler angles, which describe the relative position and orientation between the coordinates $\Gamma_c$ and $\Gamma_o$. $\delta$ is the steering angle; $\phi_f$ and $\phi_r$ are the rotating angles of the front and rear wheels, respectively. The velocity vector is

$$\mathbf{u}=[v_x\ v_y\ v_z\ \omega_x\ \omega_y\ \omega_z\ \dot{\delta}\ \dot{\phi}_r,\ \dot{\phi}_f]^T$$

whose components are quasi-velocities (generalized speeds).

### 2.2 Dynamics of the nine DOF model

For simplicity, the position, velocity and angular velocity vectors of body $M$ in frame $\Gamma_n$ will be denoted by $\mathbf{r}_M^n$, $\mathbf{v}_M^n$ and $\boldsymbol{\omega}_M^n$ respectively. One can write the position vector of point $c$ in $\Gamma_o$ as $\mathbf{r}_c^o=[X\ Y\ Z]^T$. Let the position vectors of the centers of mass of the vehicle body, rear wheel and point $e$ relative to point $c$ as $\boldsymbol{\rho}_a$, $\boldsymbol{\rho}_b$ and $\boldsymbol{\rho}_e$, respectively. That is, $\boldsymbol{\rho}_a^c=[x_a\ 0\ z_a]^T$, $\boldsymbol{\rho}_b^c=[x_b\ 0\ b_b]^T$ and $\boldsymbol{\rho}_e^c=[x_e\ 0\ z_e]^T$ in $\Gamma_c$. In a similar fashion, the position vectors $\rho_f$ and $\rho_d$ of the centers of mass of the fork and the front wheel relative to point $e$ are expressed in $\Gamma_e$ as $\rho_f^e=[x_f\ 0\ z_f]^T$ and $\rho_d^e=[x_d\ 0\ z_d]^T$.

One can write the position vectors of the centers of mass of each part in $\Gamma_o$ as

$$\begin{aligned}\mathbf{r}_a^o&=\mathbf{r}_c^o+\mathbf{R}^T\rho_a^c\\ \mathbf{r}_b^o&=\mathbf{r}_c^o+\mathbf{R}^T\rho_b^c\\ \mathbf{r}_d^o&=\mathbf{r}_c^o+\mathbf{R}^T(\rho_a^c+\mathbf{R}_{ce}^T\rho_d^e)\\ \mathbf{r}_f^o&=\mathbf{r}_c^o+\mathbf{R}^T(\rho_e^c+\mathbf{R}_{ce}^T\rho_f^e)\end{aligned}\tag{1}$$

where $\mathbf{R}$ and $\mathbf{R}_{ce}$ are the rotation matrices from $\Gamma_o$ to $\Gamma_c$ and from $\Gamma_c$ to $\Gamma_e$, respectively. These two matrices are as follows

$$\mathbf{R}=\begin{bmatrix}\cos\psi\cos\phi & \sin\psi\cos\phi & -\sin\phi\\ -\sin\psi\cos\theta+\cos\psi\sin\phi & \cos\psi\cos\theta+\sin\psi\sin\theta\sin\phi & \cos\phi\sin\theta\\ \sin\psi\sin\theta+\cos\psi\sin\phi\cos\theta & -\cos\psi\sin\theta+\sin\psi\sin\phi\cos\theta & \cos\theta\cos\phi\end{bmatrix}$$

and

$$\mathbf{R}_{ce}=\begin{bmatrix}\cos\delta & \sin\delta & 0\\ -\sin\delta & \cos\delta & 0\\ 0 & 0 & 1\end{bmatrix}\begin{bmatrix}\cos\varepsilon & 0 & -\sin\varepsilon\\ 0 & 1 & 0\\ \sin\varepsilon & 0 & \cos\varepsilon\end{bmatrix}=\begin{bmatrix}\cos\delta\cos\varepsilon & \sin\delta & -\cos\delta\sin\varepsilon\\ -\sin\delta\cos\varepsilon & \cos\delta & \sin\delta\sin\varepsilon\\ \sin\varepsilon & 0 & \cos\varepsilon\end{bmatrix}$$

The relative rotation from $\Gamma_o$ to $\Gamma_c$ is determined by the 3-2-1 Euler angles $\boldsymbol{\Phi}=[\psi\ \phi\ \theta]^T$.

The angular velocities of the vehicle body and the rear wheel are written in $\Gamma_c$ as

$$\begin{aligned}\boldsymbol{\omega}_A^c&=[\omega_x\ \omega_y\ \omega_z]^T\\ \boldsymbol{\omega}_B^c&=\boldsymbol{\omega}_A^c+\boldsymbol{\omega}_{B/A}^c=[\omega_x\ \omega_y-\dot{\phi}_r,\ \omega_z]^T\end{aligned}\tag{2}$$

where $\boldsymbol{\omega}_{B/A}^c=[0\ -\dot{\phi}_r\ 0]^T$ is the angular velocity of the rear wheel relative to the vehicle body. The vehicle body's angular velocities $\omega_z$, $\omega_y$ and $\omega_x$ are referred to as yaw, pitch and roll rates, respectively. The angular velocities are related to the time rates of the three Euler angles by the formula

$$\boldsymbol{\omega}_A=\mathbf{S}\dot{\boldsymbol{\Phi}}$$

where $\mathbf{S}=\begin{bmatrix}-\sin\phi & 0 & 1\\ \cos\phi\sin\theta & \cos\theta & 0\\ \cos\theta\cos\phi & -\sin\theta & 0\end{bmatrix}$.

The angular velocities of the fork and the front wheel can be expressed in $\Gamma_e$ as

$$\begin{aligned}\boldsymbol{\omega}_F^e&=\mathbf{R}_{ce}\boldsymbol{\omega}_A^c+\boldsymbol{\omega}_{F/A}^e\\ \boldsymbol{\omega}_D^e&=\boldsymbol{\omega}_F^e\,\boldsymbol{\omega}_{D/F}^e=\mathbf{R}_{ce}\boldsymbol{\omega}_A^c+\boldsymbol{\omega}_{F/A}^e\boldsymbol{\omega}_{D/F}^e\end{aligned}\tag{3}$$

where $\boldsymbol{\omega}_{F/A}^e=[0\ 0\ \dot{\delta}]^T$ is the angular velocity of the fork relative to the vehicle body and $\boldsymbol{\omega}_{D/F}^e=[0\ -\dot{\phi}_f\ 0]^T$ is the angular velocity of the front wheel relative to the fork.

Denote the velocity vector of point $c$ by $\mathbf{v}_c$, one has $\mathbf{v}_c^c=[v_x\ v_y\ v_z]^T$. The velocities of all parts of the vehicle are expressed as

$$\begin{aligned}\mathbf{v}_a^a&=\mathbf{v}_c^c+\boldsymbol{\omega}_A^c\times\rho_a^c\\ \mathbf{v}_b^c&=\mathbf{v}_c^c+\boldsymbol{\omega}_A^c\times\boldsymbol{\rho}_b^c\\ \mathbf{v}_d^c&=\mathbf{v}_c^c+\boldsymbol{\omega}_A^c\times\boldsymbol{\rho}_e^c+\mathbf{R}_{ce}^T(\boldsymbol{\omega}_F^e\times\boldsymbol{\rho}_d^e)\\ \mathbf{v}_f^c&=\mathbf{v}_c^c+\boldsymbol{\omega}_A^c\times\rho_e^c+\mathbf{R}_{ce}^T(\boldsymbol{\omega}_F^e\times\boldsymbol{\rho}_f^e)\end{aligned}\tag{4}$$

The kinetic energy of each part can be written in terms of centers of mass motion as

$$\begin{aligned}T_A&=\frac{1}{2}m_a(\mathbf{v}_a^c)^T\mathbf{v}_a^c+\frac{1}{2}(\boldsymbol{\omega}_A^c)^T\mathbf{I}_A\boldsymbol{\omega}_A^c\\ T_B&=\frac{1}{2}m_b(\mathbf{v}_b^c)^T\mathbf{v}_b^c+\frac{1}{2}(\boldsymbol{\omega}_B^c)^T\mathbf{I}_B\boldsymbol{\omega}_B^c\\ T_F&=\frac{1}{2}m_f(\mathbf{v}_f^c)^T\mathbf{v}_f^c+\frac{1}{2}(\boldsymbol{\omega}_F^e)^T\mathbf{I}_F\boldsymbol{\omega}_F^e\\ T_D&=\frac{1}{2}m_d(\mathbf{v}_d^c)^T\mathbf{v}_d^c+\frac{1}{2}(\boldsymbol{\omega}_D^c)^T\mathbf{I}_D\boldsymbol{\omega}_D^e\end{aligned}\tag{5}$$

**Table 1** Simulation parameters of a two-wheeled vehicle

(a)

| Name | Value | Name | Value |
|---|---|---|---|
| $m_a$ | 11.05(kg) | $m_b$ | 2.09(kg) |
| $m_d$ | 3.92(kg) | $m_f$ | 4.04(kg) |
| $\boldsymbol{\rho}_a$ | (0.1296, 0, 0.285) | $\boldsymbol{\rho}_b$ | (−0.365, 0, 0.503) |
| $\boldsymbol{\rho}_d$ | (0, 0, 0.601) | $\boldsymbol{\rho}_e$ | (−7.789, 0, 0.078) |
| $\boldsymbol{\rho}_f$ | (0.017, 0, 0.1083) | $r$ | 0.325(m) |
| $g$ | 9.80665(m/s$^2$) | $\varepsilon$ | 15° |

(b)

| | Moment of Inertia (kg·m$^2$) |
|---|---|
| Vehicle Bkody | $\mathbf{I}_a=\begin{bmatrix}0.407 & 0 & -0.068\\ & 1.934 & 0\\ & & 1.558\end{bmatrix}$ |
| Front Fork | $\mathbf{I}_f=\begin{bmatrix}0 & -0.025\\ 0.421 & 0.384 & 0\\ & & 0.041\end{bmatrix}$ |
| Wheels | $\mathbf{I}_b=\begin{bmatrix}0.109 & 0 & 0\\ & 0.218 & 0\\ & & 0.109\end{bmatrix}$ $\mathbf{I}_d=\begin{bmatrix}0.204 & 0 & 0\\ & 0.408 & 0\\ & & 0.204\end{bmatrix}$ |

where $T_A$, $T_B$, $T_F$ and $T_D$ are the kinetic energy of the vehicle body, the rear wheel, the fork and the front wheel, respectively; $\mathbf{I}_A$, $\mathbf{I}_B$, $\mathbf{I}_F$ and $\mathbf{I}_D$ are the inertia matrices of each corresponding body. Their values in our simulation are shown in Table 1. The total kinetic energy is obtained by summing all kinetic energy of all parts. By substituting the velocities in Eqs. (2), (3), (3) into (5) gives

$$T=T_A+T_B+T_F+T_D=\frac{1}{2}\mathbf{u}^T\mathbf{J}\mathbf{u}$$

where $\mathbf{J}$ is the inertia matrix of the system.

The potential energy has the form

$$V=mgh$$

or,

$$V=-\mathbf{g}_3^T(m_a\mathbf{r}_a^o+m_b\mathbf{r}_b^o+m_f\mathbf{r}_f^o+m_d\mathbf{r}_d^o)$$

where $\mathbf{g}_3=[0\ 0\ g]^T$.

The generalized velocities $\dot{\mathbf{q}}$ are related to the quasi-velocities $\mathbf{u}$ by

$$\mathbf{u}=\mathbf{Y}\dot{\mathbf{q}} \text{ or } \dot{\mathbf{q}}=\mathbf{W}\mathbf{u} \tag{6}$$

where $\mathbf{Y}$ and $\mathbf{W}$ are the 9×9 transform matrices defined by

$$\mathbf{Y}=\begin{bmatrix}\mathbf{R} & 0 & 0\\ 0 & \mathbf{S} & 0\\ 0 & 0 & \mathbf{I}\end{bmatrix},\ \mathbf{W}=\mathbf{Y}^{-1}=\begin{bmatrix}\mathbf{R}^T & 0 & 0\\ 0 & \mathbf{S}^{-1} & 0\\ 0 & 0 & \mathbf{I}\end{bmatrix}$$

and $\dot{\mathbf{q}}=[\dot{X}\ \dot{Y}\ \dot{Z}\ \dot{\psi}\ \dot{\phi}\ \dot{\theta}\ \dot{\delta}\ \dot{\phi}_r\ \dot{\phi}_f]^T$.

Lagrange's equations for quasi-coordinates can be formulated as

$$\frac{d}{dt}\left(\frac{\partial T}{\partial \mathbf{u}}\right)+\frac{\partial T}{\partial \mathbf{u}}\Delta-\frac{\partial T}{\partial \mathbf{q}}\mathbf{W}+\frac{\partial V}{\partial \mathbf{q}}\mathbf{W}=\mathbf{U}_{nc}^T \tag{7}$$

where $\frac{\partial T}{\partial \mathbf{u}}=\mathbf{u}^T\mathbf{J}$, $\frac{d}{dt}\left(\frac{\partial T}{\partial \mathbf{u}}\right)=\dot{\mathbf{u}}^T\mathbf{J}+\mathbf{u}^T\dot{\mathbf{J}}$, and $\mathbf{U}_{nc}=\mathbf{W}^T\mathbf{Q}_{nc}$ are non-conservative forces. The coefficient matrix $\Delta$ is

$$\Delta=\left(\dot{\mathbf{Y}}-\frac{\partial \mathbf{u}}{\partial \mathbf{q}}\right)\mathbf{W}=\left(\frac{d}{dt}\frac{\partial \mathbf{u}}{\partial \dot{\mathbf{q}}}-\frac{\partial \mathbf{u}}{\partial \mathbf{q}}\right)\mathbf{W}$$

where $\frac{\partial \mathbf{u}}{\partial \mathbf{q}}=\left[\frac{\partial \mathbf{u}}{\partial q_1},\ \cdots,\ \frac{\partial \mathbf{u}}{\partial q_9}\right]$.

One can rewrite Eq. (2) in the standard form of differential equations as

$$\mathbf{J}\dot{\mathbf{u}}=-\dot{\mathbf{J}}\mathbf{u}-\Delta^T\mathbf{J}\mathbf{u}+\mathbf{W}^T\left(\frac{\partial T}{\partial \mathbf{q}}\right)^T-\mathbf{W}^T\left(\frac{\partial V}{\partial \mathbf{q}}\right)^T+U$$

or simply,

$$\mathbf{J}\dot{\mathbf{u}}=\mathbf{Q} \tag{8}$$

## 3. Constraint Conditions for Wheels

In the two-wheeled vehicle model, the contact relationships between the two wheels and the ground are assumed to have the properties of rolling without slipping. The constraint equations for the rear and the front wheels are correspondingly developed as follows.

### 3.1 Rear wheel

Fig. 2 shows the schematic of the rear wheel. Let $\mathbf{R}_r$ be the position vector of contact point $o'$ relative to the center of mass $b$ of the rear wheel. The position of the contact point $o'$ is

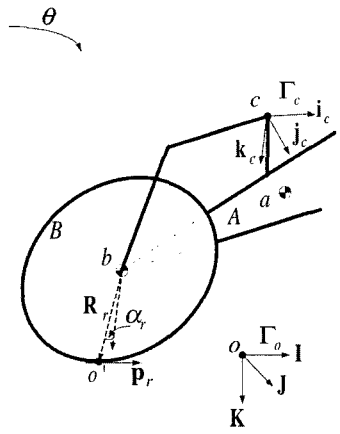


**Fig. 2** Schematic of rear wheel

$$\mathbf{r}_{o'}=\mathbf{r}_b+\mathbf{R}_r \tag{9}$$

Express Eq. (9) in $\Gamma_o$ and note that the contact point $o'$ is on the ground. The $\mathbf{K}$ component of $\mathbf{r}_{o'}^o$ is zero. This leads to a holonomic constraint

$$\begin{aligned}&Z-\sin\phi(x_b-r\sin\alpha_r)\\&\quad+\cos\phi\cos\theta(z_b+r\cos\alpha_r)=0\end{aligned} \tag{10}$$

where $\alpha_r$ is the included angle between $\mathbf{R}_r$ and $\mathbf{k}_c$, $r$ is the radius of the two wheels.

Furthermore, denote the intersecting vector between the ground and the rear wheel planes by $\mathbf{p}_r^o=[x\ y\ 0]^T$, since it is on the $\mathbf{I}-\mathbf{J}$ plane. By the observation that $\mathbf{p}_r^o$ is perpendicular to $\mathbf{j}_c$, thei r dot product is zero. That is

$$\begin{aligned}(\mathbf{R}\mathbf{p}_r^o)^T\mathbf{j}_c&=x(\cos\psi\sin\phi\sin\theta-\sin\psi\cos\theta)\\&\quad+y(\sin\psi\sin\phi\sin\theta+\cos\psi\cos\theta)\\&=0\end{aligned} \tag{11}$$

where $\mathbf{j}_c=[0\ 1\ 0]^T$.

Equation (11) gives

$$\mathbf{p}_r^o=\begin{Bmatrix}x\\y\\0\end{Bmatrix}=\begin{Bmatrix}-(\sin\psi\sin\phi\sin\theta+\cos\psi\cos\theta)\\\cos\psi\sin\phi\sin\theta-\sin\psi\cos\theta\\0\end{Bmatrix} \tag{12}$$

Similarly, $\mathbf{p}_r$ and $\mathbf{R}_r$ are perpendicular. By equating $\mathbf{p}_r\cdot\mathbf{R}_r$ (with $\mathbf{p}_r$ given in Eq. (12)) to zero yields another holonomic constraint including the extra parameter $\alpha_r$

$$\cos\phi\cos\theta\sin\alpha_r-\sin\phi\cos\alpha_r=0 \tag{13}$$

To find the nonholonomic constraint equations, we write the velocity of contact point $o'$ as

$$\mathbf{v}_{o'}=\mathbf{v}_b+\mathbf{v}_{o'/b}$$

where $\mathbf{v}_b=\mathbf{v}_c+\boldsymbol{\omega}_A\times\boldsymbol{\rho}_b$ and $\mathbf{v}_{o'/b}=\dot{\mathbf{R}}_r$. Vector $\mathbf{v}_{o'}$ can be expressed in $\Gamma_c$ as

$$\begin{aligned}\mathbf{v}_{o'}^c&=\mathbf{v}_b^c+(\dot{\mathbf{R}}_r^c)_{rel}+\boldsymbol{\omega}_B^c\times\mathbf{R}_r^c\\&=[v_{o'x}\ v_{o'y}\ v_{o'z}]^T\end{aligned} \tag{14}$$

Assume that the wheel rolls without slipping, that is $\mathbf{v}_{o'}^c=\mathbf{0}$. In $\Gamma_o$, $\mathbf{v}_{o'}$ can be written as

$$\mathbf{v}_{o'}^c=\mathbf{R}^T\mathbf{v}_{o'}^c=[v_{o'x'}\ v_{o'y'}\ y_{o'z'}]^T=\mathbf{0} \tag{15}$$

where

$$\begin{aligned}v_{o'x}&=v_{o'x}(\cos\psi\cos\phi)\\&\quad+v_{o'y}(\cos\psi\sin\phi\sin\theta-\sin\psi\cos\theta)\\&\quad+v_{o'z}(\cos\psi\sin\phi\cos\theta+\sin\psi\sin\theta)\end{aligned} \tag{16}$$

$$\begin{aligned}v_{o'y}&=v_{o'x}(\sin\psi\cos\phi)\\&\quad+v_{o'y}(\sin\psi\sin\phi\sin\theta+\cos\psi\cos\theta)\\&\quad+v_{o'z}(\sin\psi\sin\phi\cos\theta+\cos\psi\sin\theta)\end{aligned} \tag{17}$$

$$\begin{aligned}v_{o'z'}=&-v_{o'x}\sin\phi+v_{o'y}\cos\phi\sin\theta\\&+v_{o'z}\cos\phi\cos\theta\end{aligned} \tag{18}$$

It appears that the constraint $v_{o'z'}=0$ is proved to be an integrable equation, which can be obtained by differentiating Eqs. (10) and (13). Therefore, Eq. (18) is trivial since it is only a velocity form of the holonomic constraint. Thus, from Eqs. (16) and (17) we only have two nonholonomic constraints

$$\begin{aligned}&v_{o'x}(\cos\psi\cos\phi)+v_{o'y}(\cos\psi\sin\phi\sin\theta-\sin\psi\cos\theta)\\&+v_{o'z}(\cos\psi\sin\phi\cos\theta+\sin\psi\sin\theta)=0\end{aligned}$$

$$\begin{aligned}&v_{o'x}(\sin\psi\cos\phi)+v_{o'y}(\sin\psi\sin\phi\sin\theta-\cos\psi\cos\theta)\\&+v_{o'z}(\sin\psi\sin\phi\cos\theta+\cos\psi\sin\theta)=0\end{aligned}$$

### 3.2 Front wheel

The constraint conditions of the front wheel can be obtained by the same procedures as those used with the rear wheel. Vector $\mathbf{R}_f$ is used to designate the position of the center of mass $d$ of the wheel relative to the contact point $s$. The position of the contact point $s$ is

$$\mathbf{r}_s=\mathbf{r}_d+\mathbf{R}_f \tag{19}$$

Writing Eq. (19) in $\Gamma_o$ and equating the $\mathbf{K}$ component of $\mathbf{r}_s^o$ to zero gives a holonomic constraint

$$
\begin{aligned}
&Z-x_e\sin\phi+z_e\cos\phi\cos\theta+z_d(-\sin\phi\sin\varepsilon+\cos\phi\cos\theta\cos\varepsilon)\\
&+x_d(-\sin\phi\cos\delta\cos\varepsilon+\cos\phi\sin\theta\sin\delta-\cos\phi\cos\theta\cos\delta\sin\varepsilon)\\
&+r\sin\alpha_f(-\cos\phi\sin\theta\sin\delta+\cos\delta\\
&\qquad+\cos\phi\cos\theta\cos\delta\sin\varepsilon+\sin\phi\cos\delta\cos\varepsilon)\\
&+r\cos\alpha_f(-\sin\phi\sin\varepsilon+\cos\phi\cos\theta\cos\varepsilon)=0
\end{aligned}
\tag{20}
$$

where $\alpha_f$ is the included angle between $\mathbf{R}_f$ and $\mathbf{k}_e$.

The intersecting vector between the ground and the front wheel planes, $\mathbf{p}_f$, can be obtained by equating $\mathbf{p}_f\cdot\mathbf{j}_e$ to zero, that gives

$$
\mathbf{p}_p^o=\begin{Bmatrix}x\\y\\0\end{Bmatrix}
=\begin{Bmatrix}
-\left(\begin{array}{l}\cos\delta(\sin\psi\sin\phi\sin\theta+\cos\psi\cos\theta)-\sin\psi\cos\phi\sin\delta\cos\varepsilon\\+\sin\delta\sin\varepsilon(\sin\psi\sin\phi\cos\theta-\cos\psi\sin\theta)\end{array}\right)\\
\cos\delta(\cos\psi\sin\phi\sin\theta-\sin\psi\cos\theta)-\cos\psi\cos\phi\sin\delta\cos\varepsilon\\
+\sin\delta\sin\varepsilon(\cos\psi\sin\phi\cos\theta+\sin\psi\sin\theta)\\
0
\end{Bmatrix}
\tag{21}
$$

Another holonomic constraint can be found by performing $\mathbf{p}_f\cdot\mathbf{R}_f=0$. That gives

$$
\begin{aligned}
&(\cos\phi\sin\theta\sin\delta-\cos\phi\cos\theta\cos\delta\sin\varepsilon\\
&-\sin\phi\cos\delta\cos\varepsilon)\cos\alpha_f\\
&+(\cos\phi\cos\theta\cos\varepsilon-\sin\phi\sin\varepsilon)\sin\alpha_f=0
\end{aligned}
\tag{22}
$$

To find the nonholonomic constraints of the front wheel, we express the velocity of the contact point $s$ as follows

$$\mathbf{v}_s=\mathbf{v}_e+\mathbf{v}_{d/e}+\mathbf{v}_{s/d}$$

where $\mathbf{v}_e=\mathbf{v}_c+\boldsymbol{\omega}_A\times\boldsymbol{\rho}_e$, $\mathbf{v}_{d/e}=\boldsymbol{\omega}_F\times\boldsymbol{\rho}_d$, and $\mathbf{v}_{s/d}=\dot{\mathbf{R}}_f$, Vector $\mathbf{v}_s$ can be written in $\gamma_e$ as

$$
\begin{aligned}
\mathbf{v}_s^c&=\mathbf{v}_c^c+\boldsymbol{\omega}_A^c\boldsymbol{\rho}_e^c+\mathbf{R}_{ce}^T(\boldsymbol{\omega}_F^e\times\rho_d^e)\\
&\quad+(\dot{\mathbf{R}}_f^e)_{rel}+\mathbf{R}_{ce}^T(\omega_D^e+\mathbf{R}_f^e)\\
&=[v_{xx}\ v_{sy}\ v_{sz}]^T
\end{aligned}
\tag{23}
$$

With the assumption of non-slip rolling of the wheel and zero-velocity motion of the contact point $s$, one has $\mathbf{v}_s^c=\mathbf{0}$. Furthermore, in $\Gamma_o$, Eq. (23) becomes

$$\mathbf{v}_s^o=\mathbf{R}^T\mathbf{v}_s^c=[v_{sx'}\ v_{sy'}\ v_{sz'}]^T$$

where

$$
\begin{aligned}
v_{sx'}&=v_{sx}\cos\psi\cos\phi\\
&\quad+v_{sy}(\cos\psi\sin\phi\sin\theta-\sin\psi\cos\theta)\\
&\quad+v_{sz}(\cos\psi\sin\phi\cos\theta+\sin\psi\sin\theta)
\end{aligned}
\tag{24}
$$

$$
\begin{aligned}
v_{sy'}&=v_{sx}\sin\psi\cos\phi\\
&\quad+v_{sy}(\sin\sin\phi\sin\theta+\cos\psi\cos\theta)\\
&\quad+v_{sz}(\sin\psi\sin\phi\cos\theta+\cos\psi\sin\theta)
\end{aligned}
\tag{25}
$$

$$
\begin{aligned}
v_{sz'}&=-v_{sx}\sin\phi+v_{sy}\cos\phi\sin\theta\\
&\quad+v_{sz}\cos\phi\cos\theta
\end{aligned}
\tag{26}
$$

It is also proved that Eq. (26) can be obtained by differentiating Eqs. (20) and (22). Hence, Eqs. (24) and (25) give two nonholonomic constraints

$$
\begin{aligned}
&v_{sx}\cos\psi\cos\phi+v_{sy}(\cos\psi\sin\phi\sin\theta-\sin\psi\cos\theta)\\
&+v_{sz}(\cos\psi\sin\phi\cos\theta+\sin\psi\sin\theta)=0
\end{aligned}
$$

$$
\begin{aligned}
&v_{sx}\sin\psi\cos\phi+v_{sy}(\sin\psi\sin\phi\sin\theta+\cos\psi\cos\theta)\\
&+v_{sz}(\sin\psi\sin\phi\cos\theta-\cos\psi\sin\theta)=0
\end{aligned}
$$

### 3.3 Constraint Jacobian matrix

As a result, eight constraints are obtained in Eqs. (10), (13), (16), (17), (20), (22), (24) and (25). Among these, there are four holonomic and four nonholonomic constraints. To derive the constraint equations, two algebraic variables, $\alpha_r$ and $\alpha_f$, were introduced. Hence, the generalized coordinate and quasi-velocity vectors are expanded to

$$\mathbf{q}_e=[X\ Y\ Z\ \psi\ \phi\ \delta\ \theta\ \phi_r\ \phi_f\ \alpha_r\ \alpha_f]^T$$

$$\mathbf{U}=[v_x\ y_y\ v_z\ \omega_x\ \omega_y\ \omega_z\ \dot{\delta}\ \dot{\phi}_r\ \dot{\phi}_f\ \dot{\alpha}_r\ \dot{\alpha}_f]^T$$

Differentiate all the holonomic constraints to yield the velocity form, which with other nonholonomic constraints can be written as

$$\mathbf{BU}=\mathbf{0} \tag{27}$$

where $\mathbf{B}$ is an $8\times11$ matrix, referred to as constraint Jacobian matrix. The equations of motion with constraint conditions now become

$$
\begin{cases}
\dot{\mathbf{q}}_e=\mathbf{W}_e\mathbf{U}\\
\mathbf{J}_e\dot{\mathbf{U}}=\mathbf{Q}_e+\tau-\mathbf{B}^T\boldsymbol{\lambda}\\
\mathbf{BU}=\mathbf{0}
\end{cases}
\tag{28}
$$

where $\mathbf{W}_e=\begin{bmatrix}\mathbf{W}&\mathbf{0}&\mathbf{0}\\\mathbf{0}&1&0\\\mathbf{0}&0&1\end{bmatrix}$ is an $11\times11$ matrix, $\mathbf{J}_e=\begin{bmatrix}\mathbf{J}&\mathbf{0}&\mathbf{0}\\\mathbf{0}&0&0\\\mathbf{0}&0&0\end{bmatrix}$ is an $11\times11$ generalized mass matrix, $\mathbf{Q}_e=\begin{Bmatrix}\mathbf{Q}\\0\\0\end{Bmatrix}$ is vector of applied forces, $\boldsymbol{\lambda}$

represents the eight Lagrange multipliers or constraint forces coupled to the system by the $8\times11$ constraint Jacobian matrix $\mathbf{B}$, and $\boldsymbol{\tau}$ is the generalized nonconservative force vector.

## 4. Equilibrium of Two-Wheeled Vehicles

Equilibrium is an essential and very useful concept in dynamics. For a multibody dynamic system, equilibrium is defined as the state when the total force acting on the system is zero (Baruh, 1999). For a two-wheeled vehicle system, equilibrium is necessary to understand its interesting dynamic behaviors and to control the vehicle to follow a given circular path or a straight line.

This section discusses an important question coming to mind when dealing with the equilibrium of two-wheeled vehicles on : How to calculate the equilibrium points of two-wheeled vehicles' dynamics.

### 4.1 Equilibrium points searching strategy

To calculate the equilibrium points of a two-wheeled vehicle system one can utilize the constraint equations to compute the state variables when the system is at equilibrium. Equation (28) suggests that

$$\mathbf{J}_e\dot{\mathbf{U}}=\mathbf{Q}_e+\boldsymbol{\tau}-\mathbf{B}^T\boldsymbol{\lambda} \tag{29}$$

Practice shows that only the steering torque is needed to control the vehicle to an equilibrium point. Therefore, in the force vector $\boldsymbol{\tau}$, only the seventh element, the steering torque $\tau_s$ is nonzero is necessary. That is $\boldsymbol{\tau}=[0, \cdots, 0, \tau_s, 0, \cdots, 0]^T$. Two-wheeled vehicle dynamics and the computation of constraint equations are implemented in numerical simulations. In order to eliminate the Lagrange multipliers in the constraint equations, Eq. (29) is multiplied by the orthogonal complement of matrix $\mathbf{B}$, matrix $\mathbf{T}$, so that $\mathbf{TB}^T=\mathbf{0}$. Equation (29) thus becomes

$$\mathbf{TJ}_e\dot{\mathbf{U}}=\mathbf{TQ}_e+\mathbf{T}\boldsymbol{\tau} \tag{30}$$

It is clear that all the state variables must satisfy the constraint equations. However, it appears that the constraint equations are independent of the variables $X$, $Y$, $\psi$, $\phi_r$ and $\phi_f$ ; and at equilibrium state : $\dot{\delta}=\dot{\alpha}_r=\dot{\alpha}_f=0$. Therefore, there are still fourteen among totally twenty-two state variables to be determined. The four holonomic constraints in Eqs. (10), (13), (20) and (22) can be derived to yield their time rates, which are also constraint equations. Hence, there are totally twelve constraint equations.

The Newton's second law can be used to calculate the equilibrium points of the system by setting the acceleration term in Eq. (30) to zero. The constraint condition thus is defined as

$$\mathbf{TQ}_e+\mathbf{T}\boldsymbol{\tau}=\mathbf{0} \tag{31}$$

The searching steps for equilibrium points then can be summarized as follows

(1) Given $\theta$, change the value of $v_x$ in a certain range, e.g., $v_0\leq v_x\leq v_1$. For each pair of $(\theta,\ v_x)$, solve for all the state variables and calculate the two matrices $\mathbf{B}$ and $\mathbf{Q}_e$.

(2) Compute the orthogonal complement matrix $\mathbf{T}$ from $\mathbf{B}$ : there are a number of methods to calculate $\mathbf{T}$, the Pseudo Upper Triangular Decomposition Method (Amirouche, 1992) is one of them.

(3) Verify whether Eq. (31) is satisfied.

Simulation results show that, even at equilibrium state, there still exists a small amount of steering torque $\tau_s$ to maintain the vehicle's stabilization. It is reasonable because this torque is necessary to counteract the self-aligning torque, which tends to align the wheel plane with the direction of motion when the angles $\alpha_r$ and $\alpha_f$ are nonzero.

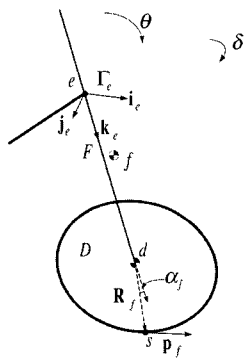


**Fig. 3** Schematic of front wheel

The searching results are selectively shown in Table 2. These are unstable equilibrium points, that is, when the vehicle moves away from an equilibrium state, it never returns without a controller. Fig. 7 shows the relationship between $v_x$ and the steering angle $\delta$ when the vehicle is at equilibrium with constant $\theta$ angles. Fig. 7 indicates that with a constant $\theta$, $\delta$ decreases when $v_x$ increases. At high speeds, the change in the slope of the curves is much milder than it is at low speeds.

**Table 2** Selected equilibrium points

| $\theta$ (deg) / States | 10 | 15 | 20 | 25 |
|---|---|---|---|---|
| $\dot{X}$ (km/h) | NAC | NAC | NAC | NAC |
| $\dot{Y}$ (km/h) | NAC | NAC | NAC | NAC |
| $\dot{Z}$ (km/h) | 0 | 0 | 0 | 0 |
| $v_x$ (km/h) | 10.283 | 9.552 | 8.371 | 6.611 |
| $v_y$ (km/h) | 0.750 | 1.168 | 1.568 | 2.065 |
| $v_z$ (km/h) | −0.167 | −0.373 | −0.657 | −1.065 |
| $\dot{\psi}$ (rad/s) | 0.581 | 0.906 | 1.291 | 1.798 |
| $\dot{\phi}$ (rad/s) | 0 | 0 | 0 | 0 |
| $\dot{\theta}$ (rad/s) | 0 | 0 | 0 | 0 |
| $\dot{\delta}$ (rad/s) | 0 | 0 | 0 | 0 |
| $\dot{\phi}_r$ (rad/s) | −9.051 | −8.772 | −8.289 | −7.608 |
| $\dot{\phi}_f$ (rad/s) | −9.390 | −9.574 | −10.148 | −11.085 |
| $\alpha_r$ (rad/s) | 0 | 0 | 0 | 0 |
| $\alpha_f$ (rad/s) | 0 | 0 | 0 | 0 |
| $X$ (m) | NAC | NAC | NAC | NAC |
| $Y$ (m) | NAC | NAC | NAC | NAC |
| $Z$ (m) | −0.813 | −0.796 | −0.774 | −0.747 |
| $\psi$ (deg) | NAC | NAC | NAC | NAC |
| $\phi$ (deg) | −0.175 | −0.329 | −0.424 | −0.562 |
| $\theta$ (deg) | 10 | 15 | 20 | 25 |
| $\delta$ (deg) | 14.739 | 22.542 | 31.157 | 41.731 |
| $\phi_r$ (deg) | NAC | NAC | NAC | NAC |
| $\phi_f$ (deg) | NAC | NAC | NAC | NAC |
| $\alpha_r$ (deg) | −0.178 | −0.341 | −0.452 | −0.366 |
| $\alpha_f$ (deg) | 11.787 | 7.615 | 1.450 | −7.355 |
| $\tau_s$ (N-m) | −0.0931 | −0.0745 | −0.0201 | −0.0010 |
| $R_c$ (m) | 4.9418 | 2.9514 | 1.8459 | 1.0745 |

NAC stands for "Not a constant".

### 4.2 Radii of curvatures

Fig. 4 shows a trajectory of the vehicle at an equilibrium point. This trajectory is a circular path. Simply by using geometric relationships, the radius of any trajectory of two-wheeled vehicles can be computed.

Let $o'$, $s$ be the contact points of the rear and the front wheels with the ground, respectively, and $c$ be the reference point, as shown in Fig. 1 (b). The radii of curvatures of points $o'$, $s$ and $c$ of the given two-wheeled vehicle system at any position are diagrammatized in Fig. 5. It appears that these three points are on three different

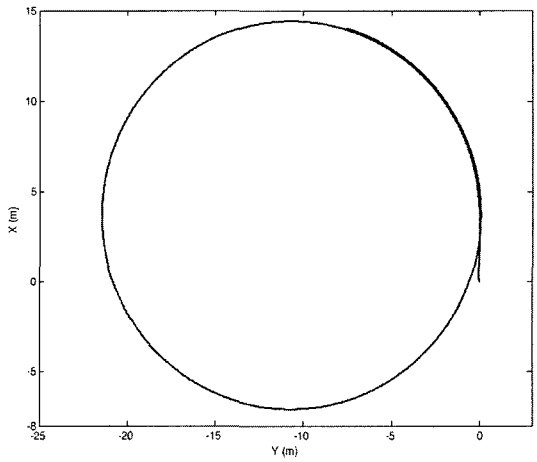


**Fig. 4** Trajectory of two-wheeled vehicle at equilibrium

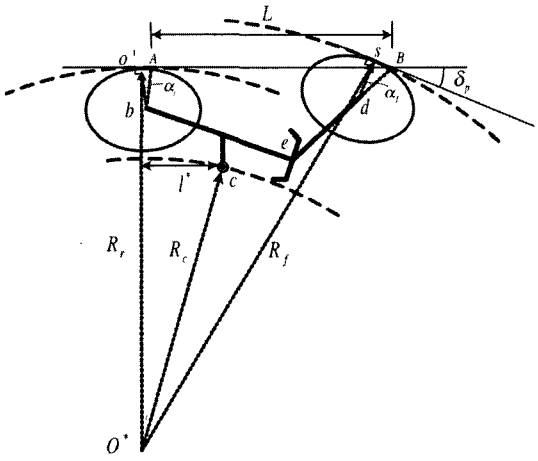


**Fig. 5** Radii of curvatures

curvatures, but share one common center, this point is designated by $O^*$ in Fig. 5. Let $\delta_p$ be the projection of the steering angle $\delta$ on the ground. This leads to

$$\delta_p=\text{sign } \delta\times\cos^{-1}\left(\frac{\mathbf{p}_r\cdot\mathbf{p}_f}{|\mathbf{p}_r|\times|\mathbf{p}_f|}\right) \tag{32}$$

where $\mathbf{p}_r$ and $\mathbf{p}_f$ are the intersecting vectors of the ground with the rear and the front wheel planes, respectively, as shown in Fig. 2 and Fig. 3.

In Fig. 5, let $A$ be the contact point of the rear wheel with the ground when $\theta=0$, $B$ be the intersection of the extended line of the fork with the ground. Let $h_c>0$ be the distance from the reference point $c$ to the ground when $\theta=0$. One has

$$L=AB=-x_b+x_e+(h_c-z_e)\tan\varepsilon \tag{33}$$

where $\varepsilon$ is the rake angle of the fork and $r$ is the radius of the two wheels. Their values are given in Table 1. One should note that $x_b$ and $x_e$ are negative constants.

The distance from $o'$ to $B$ is given by

$$L_r=o'B=L+r\sin\alpha_r \tag{34}$$

and the distance from $s$ to $B$ is

$$L_f=sB=r\sin\alpha_f \tag{35}$$

From Fig. 6, the radius of curvature of point $o'$ on the rear wheel thus can be formulated as

$$R_r=\frac{L_r-\dfrac{L_f}{\cos\delta_p}}{\tan\delta_p}=\frac{L+r\sin\alpha_r-r\dfrac{\sin\alpha_f}{\cos\delta_p}}{\tan\delta_p} \tag{36}$$

the radius of curvature of point $s$ on the front wheel

$$\begin{aligned}R_f&=\frac{L_r-\dfrac{L_f}{\cos\delta_p}}{\sin\delta_p}+L_f\tan\delta_p\\&=\frac{L+r\sin\alpha_r-r\dfrac{\sin\alpha_f}{\cos\delta_p}}{\sin\delta_p}+r\sin\alpha_f\tan\delta_p\end{aligned} \tag{37}$$

and the radius of curvature of the reference point $c$

$$\begin{aligned}R_c&=\frac{R_r-h_c\sin\theta}{\cos\left[\tan^{-1}\left(\dfrac{l^*}{R_r-h_c\sin\theta}\right)\right]}\\&=\frac{R_r-h_c\sin\theta}{\cos\left[\tan^{-1}\left(\dfrac{-x_b+r\sin\alpha_r}{R_r-h_c\sin\theta}\right)\right]}\end{aligned} \tag{38}$$

where $l^*=-x_b+r\sin\alpha_r$.

The relationship between $v_x$, $\delta$ and $R_c$ when the vehicle is at equilibrium is plotted in Fig. 8.

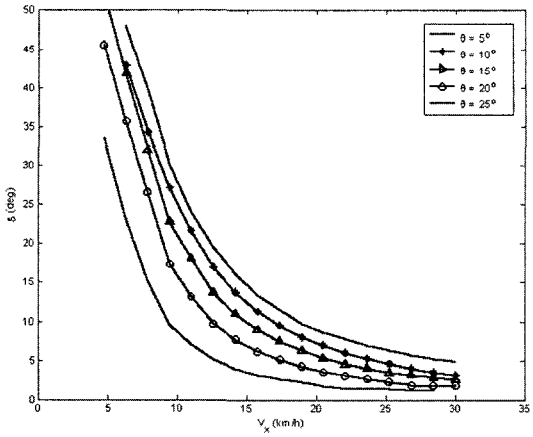


**Fig. 7** Relationship between $v_x$ and $\delta$ with constant $\theta$

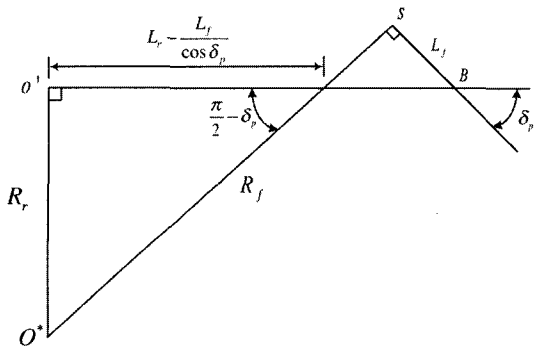


**Fig. 6** Determine $R_r$ and $R_f$

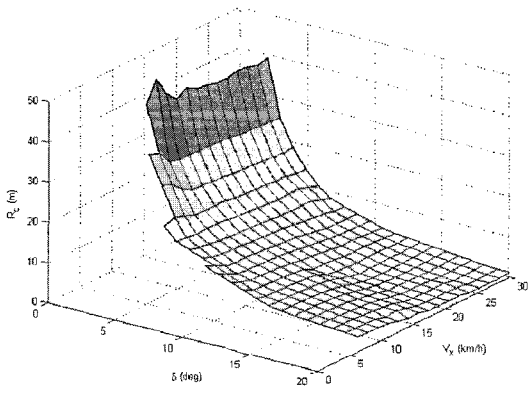


**Fig. 8** Relationship between $v_x$, $\delta$ and $R_c$

It can be seen that the radius $R_c$ seems to be dependent on the steering angle only, the velocity $v_x$ has very little effect on $R_c$. It is what we expected, because the radii of curvatures of the vehicle are only dependent on the steering angle $\delta$ and the roll angle $\theta$, which are proved in Eqs. (36), (37) and (38). A change in $v_x$ can lead to a change in $\theta$, but $\theta$ does not influence $R_c$ very much.

## 5. Conclusions

In this paper, a nine DOF dynamic model of two-wheeled vehicles is developed using Lagrange's equations for quasi-coordinates. Considering the contact relationship between the wheels and the ground surface, the constraint conditions, including four holonomic and four nonholonomic constraints, can be derived. By combining the nonholonomic constraints and the velocity forms of holonomic constraints, the constraint Jacobian matrix can be obtained. With the developed equations of motion and constraints, the equilibrium of two-wheeled vehicles can be fully investigated. The dynamic model in this study provides a fundamental in understanding the interesting dynamic behaviors of two-wheeled vehicles. With this model, one can also implement simulations, design controllers and do experiments.

## Acknowledgment

The authors would like to thank the National Science Council of the Republic of China, Taiwan, for financially supporting the research under project number NSC 92-2213-E-212-006.

## References

Alleyne, A. and DePoorter, M., 1997, "Lateral Displacement Sensor Placement and Forward Velocity Effects on Stability of Lateral Control of Vehicles," *American Control Conference*, Vol. 3, pp. 1593~1597.

Amirouche, F. M. L., 1992, Computational Methods in Multibody Dynamics, Prentice-Hall.

Baruh, H., 1999, Analytical Dynamics, McGraw-Hill.

Beznos, A. V., Formal'sky, A. M., Gurfinkel, E. V., Jicharev, D. N., Lensky, A. V., Savitsky, K. V. and Tchesalin, L. S., 1998, "Control of Autonomous Motion of Two-wheel Bicycle with Gyroscopic Stabilisation," *Proceedings of the 1998 IEEE International Conference on Robotics & Automation*, Leuven, Belgium May, Vol. 3, pp. 2670~2675.

Chen, C. and Tan, H. S., 1998, "Steering Control of High Speed Vehicles: Dynamic Look Ahead and Yaw Rate Feedback," *Proceedings of the 37th IEEE Conference on Decision & Control*, Tampa, Florida USA.

Feng, K. T., Tan, H. S. and Tomizuka, M., 1998, "Automatic Steering Control of Vehicle Lateral Motion with the Effect of Roll Dynamics," *Proceedings of the American Control Conference*, Philadelphia, Pennsylvania.

Getz, N. H., 1993, "Control of Nonholonomic Systems With Dynamically Decoupled Actuators," *Proceedings of the 32nd Conference on Decision and Control*, San Antonio, Texas.

Getz, N. H., 1994, "Control of Balance for a Nonlinear Nonholonomic Non-minimum Phase Model of a Bicycle," *Proceedings of the American Control Conference*, Baltimore, Maryland.

Getz, N. H., 1995, "Internal Equilibrium Control of a Bicycle," *Proceedings of the 34th Conference on Decision & Control*, New Orleans, LA-December, Vol. 4, pp. 4286~4287.

Getz, N. H. and Hedrick, J. K., 1995, "An Internal Equilibrium Manifold Method of Tracking for Nonlinear Nonminimum Phase Systems," *Proceedings of the American Control Conference*, Seattle, Washington.

Getz, N. H. and Marsden, J. E., 1995, "Control for an Autonomous Bicycle," *IEEE International Conference on Robotics and Automation*, Vol. 2, pp. 1397~1402.

Indiveri, G., 1999, "Kinematic Time-invariant Control of a 2D Nonholonomic Vehicle," *Proceedings of the 38th IEEE Conference on Decision & Control*, Vol. 3, pp. 2112~2117.

Lee, S. and Ham, W., 2002, "Self Stabilizing Strategy in Tracking Control of Unmanned Electric Bicycle with Mass Balance," *IEEE/RSJ In-*

*ternational Conference on Intelligent Robots and System*, Vol. 3, pp. 2200~2205.

Suryanarayanan, S., Tomizuka, M. and Weaver, M., 2002, "System Dynamics and Control of Bicycles at High Speeds," *American Control Conference*, Vol. 2, pp. 845~850.

Yao, Y. S. and Chellappa, R., 1994, "Estimation of Unstabilized Components in Vehicular Motion," *Proceedings of the 12th IAPR International Conference on Computer Vision & Image Processing*, Vol. 1, pp. 641-644.

Yavin, Y., 1997, "Navigation and Control of the Motion of a Riderless Bicycle by Using a Simplified Dynamic Model," *Mathematical and Computer Modelling*, Vol. 25, pp. 67~74.

Yavin, Y., 1998, "Navigation and Control of the Motion of a Riderless Bicycle," *Compute. Methods Appl. Mech. Engrg.*, 160, pp. 193~202.

Yavin, Y., 1999, "Stabilization and Control of the Motion of an Autonomous Bicycle by Using a Rotor for the Tilting Moment," *Computer Methods in Applied Mechanics and Engineering*, Vol. 178, pp. 233~243.